frontiers in Earth Science

ORIGINAL RESEARCH
published: 16 November 2016
doi: 10.3389/feart.2016.00098

Disentangling Natural and Anthropogenic Signals in Lacustrine Records: An Example from the Ilan Plain, NE Taiwan

Jyh-Jaan Huang[1], Chih-An Huh[2†], Kuo-Yen Wei[1], Ludvig Löwemark[1], Shu-Fen Lin[3], Wen-Hsuan Liao[4,5], Tien-Nan Yang[6], Sheng-Rong Song[1], Meng-Yang Lee[7], Chih-Chieh Su[8] and Teh-Quei Lee[2]*

[1] *Department of Geosciences, National Taiwan University, Taipei, Taiwan,* [2] *Institute of Earth Sciences, Academia Sinica, Taipei, Taiwan,* [3] *Institute of History and Philology, Academia Sinica, Taipei, Taiwan,* [4] *Research Center for Environmental Changes, Academia Sinica, Taipei, Taiwan,* [5] *Earth System Science Program, Taiwan International Graduate Program, Academia Sinica, Taipei, Taiwan,* [6] *Exploration and Development Research Institute, CPC Corporation, Miaoli, Taiwan,* [7] *Department of Earth and Life Science, University of Taipei, Taipei, Taiwan,* [8] *Institute of Oceanography, National Taiwan University, Taipei, Taiwan*

OPEN ACCESS

Edited by:
Gary E. Stinchcomb, Murray State University, USA

Reviewed by:
Li Wu, Anhui Normal University, China
Maarten Blaauw, Queen's University Belfast, UK
Samuel Munoz, Woods Hole Oceanographic Institution, USA

***Correspondence:**
Ludvig Löwemark
loewemark@gmail.com

[†] *Deceased, Jan. 21st, 2014.*

Specialty section:
This article was submitted to Quaternary Science, Geomorphology and Paleoenvironment, a section of the journal Frontiers in Earth Science

Received: *24 August 2016*
Accepted: *31 October 2016*
Published: *16 November 2016*

Citation:
Huang J-J, Huh C-A, Wei K-Y, Löwemark L, Lin S-F, Liao W-H, Yang T-N, Song S-R, Lee M-Y, Su C-C and Lee T-Q (2016) Disentangling Natural and Anthropogenic Signals in Lacustrine Records: An Example from the Ilan Plain, NE Taiwan. Front. Earth Sci. 4:98. doi: 10.3389/feart.2016.00098

The impact of human activities has been increasing to a degree where humans now outcompete many natural processes. When interpreting environmental and climatic changes recorded in natural archives on historical time scales, it is therefore important to be able to disentangle the relative contribution of natural and anthropogenic processes. Lake Meihua on the Ilan Plain in northeastern Taiwan offers a particularly suitable opportunity to test how human activities known from historical records can be recorded in lacustrine sediment. For this purpose, three cores from Lake Meihua have been studied by a multiproxy approach, providing the first decadal-resolution lacustrine records covering the past 150 years in Taiwan. Profiles of excess ^{210}Pb, ^{137}Cs and ^{239,240}Pu from two short cores (MHL-09-01 and MHL-11-02) allowed a precise chronology to be established. The presence of a yellow, earthy layer with lower levels of organic material coincide with the record of land development associated with the construction of the San-Chin-Gong Temple during AD 1970–1982. Furthermore, in the lower part of the cores, the upwards increasing trend of inc/coh, TOC, TOC/TN, and grain size, coupled with the palynological data (increase of *Alnus, Mallotus, Trema* and herbs) from the nearby core MHL-5A with radiocarbon chronology, suggest that the area surrounding the lake has been significantly affected by agricultural activities since the arrival of Chinese settlers around ~AD 1874. In sum, this study demonstrates that this suite of lacustrine sediments in northeastern Taiwan has recorded human activities in agreement with historical documents, and that different human activities will leave distinct sedimentological, geochemical, and palynological signatures in the sedimentary archives. Therefore, multiproxy reconstructions are important to capture the complex nature of human-environmental interactions. A better understanding of the weathering and erosion response to human activities can also provide useful information for sustainable land-use management.

Keywords: human activities, radionuclides, XRF core scanner, environmental change, organic indicators, pollen

INTRODUCTION

Over the course of the Holocene, the environmental impact of human activities has gradually come to overshadow the impact of natural processes (Montgomery, 2007; Syvitski and Kettner, 2011). These anthropogenic environmental alterations have caused accelerated erosion of land cover to produce anthropogenic sediments (also known as legacy sediments; James, 2013). The erosion, transportation, and re-sedimentation of anthropogenic sediments have attracted increasingly more attention, both because of the need to separate the anthropogenic imprints from natural signals when studying past climatic changes, and because these legacy sediments contain records of the interaction between human society and the environment (James, 2013).

Taiwan, a small island situated on the western margin of the Pacific Ocean covers an area of only 35,980 km^2 with a population over 23 million. The heavy population density (642 people/km^2, 16^{th} in the world) and rapid land-development in recent history should make Taiwan an ideal location to study the influence of anthropogenic processes (Huang and Lin, 2003; Chen et al., 2007a). However, the rapid uplift, steep topography, and high erosion rates up to 3–6 mm yr^{-1} in Taiwan (Dadson et al., 2003) make it difficult to study historical human-environment interactions. Therefore, in Taiwan, millennial to centennial-scale climatic oscillations have only been studied through palynological and geochemical proxies from a limited number of lakes (Wang et al., 2011; Yang et al., 2011b, 2014; Chen et al., 2012; Liew et al., 2014), and even fewer studies have been conducted on human-environment interactions on historical/archaeological time scales due to the scarcity of high resolution material (Lin et al., 2007; Yang et al., 2014).

Unlike other places in Taiwan where uplift is dominating, the Ilan Plain in northeastern Taiwan is characterized by tectonic subsidence which is the result of the westward propagation of the Okinawa Trough (Shyu et al., 2005; **Figure 1A**). Consequently, the subsiding Ilan Plain has acted as a depocenter for sediments delivered by the Lanyang River (the main river system on the Ilan Plain) and has accumulated over 120 m of sediments since last glacial maximum (LGM) (Wei et al., 2003; Chen et al., 2009). Lake Meihua, located at the southern edge of Ilan Plain, has received massive amounts of suspended material from its local drainage and/or nearby local river systems by overbank deposits (**Figures 1A,B**). Previous studies have shown that these sediments can provide exquisite lacustrine records for the study of paleoenvironmental changes during the Holocene (Chen et al., 2012).

Developing reliable proxy records of anthropogenic impact on the environment is difficult for two reasons. First, the changes are often considerably more abrupt and rapid than their natural counterparts, requiring high-resolution techniques and materials, and second, the relation between human activities and the signals recorded in the sedimentary archives are often poorly understood. To overcome these obstacles, we make use of the fast and non-destructive micro X-ray fluorescence (XRF) scanning technique (Croudace et al., 2006; Huang et al., 2016) that can deliver the radiographic images, elemental variations and organic-related incoherent over coherent ratios (inc/coh) directly from the untreated sediments at sub-mm resolution (Guyard et al., 2007; Rolland et al., 2008; Sáez et al., 2009; Brunschön et al., 2010) to analyze the records of rapid anthropogenic impacts preserved in the sedimentary archives (Miller et al., 2014). Moreover, the well-documented and relatively uncomplicated settlement and development history on the Ilan Plain offers a particularly suitable opportunity to test how human activities known from historical records have been recorded in the lacustrine sediment.

The aim of this study is to assess how known human activities are recorded in the sedimentary archives of a confined lake basin. Therefore, three cores from Lake Meihua have been studied by multi-geochemical and palynological proxies, and address the anthropogenic impacts covering the past 150 years in northern Taiwan. A better understanding of how human activities are recorded in the sedimentary archives is of imperative importance to disentangle natural and anthropogenic signals, and may also provide useful information for land-use management and sustainable environment governance.

STUDY AREA

Geological Background

The lacustrine cores used in this study were retrieved from Lake Meihua (121° 43.57′, 24° 38.35′; 52 ha; 50 m a.s.l.), which is situated on the southern edge of the Ilan Plain, northeastern Taiwan. The Ilan Plain is a triangular-shaped alluvial-fan delta, facing the Pacific Ocean to the east. Two major mountain ranges border the northern and southern flanks, the Hsueshan Range and the Central Range, respectively (**Figure 1A**). The basement rock here is mainly composed of Tertiary argillite, slate and metasandstone (Ho, 1986). The continuous subsidence associated with the westward propagation of the Okinawa Trough has provided over 120 m of sedimentary accommodation space in the Ilan basin since the LGM (Wei et al., 2003; Chen et al., 2009). The high sedimentation rates are the result of intense rain-induced erosion of surrounding mountain areas; the Lanyang River supplies about 17 Mt of suspended sediments per year (Dadson et al., 2003). The position at the southern edge of the Ilan Plain results in Lake Meihua being surrounded by hills, with the only opening toward the Ilan Plain to the north (**Figure 1B**). A normal faulting system relating to the tectonic subsidence along the mountain front (Shyu et al., 2005) together with rapid river aggradation at the northern shore of the lake has allowed the lake to persist for an unusually long time, preserving an exquisite lacustrine record since at least the mid-Holocene (Chen et al., 2012).

Climate and Vegetation

The climate of the Ilan area is humid and subtropical, influenced by both the East Asian summer and winter monsoons, with frequent typhoon activities in summer and autumn. The annual mean temperature is ∼22.2°C and the average annual precipitation over past 50 years is roughly 2760 mm (Central Weather Bureau, www.cwb.gov.tw). The natural vegetation in the study area mainly consists of subtropical evergreen rainforest,

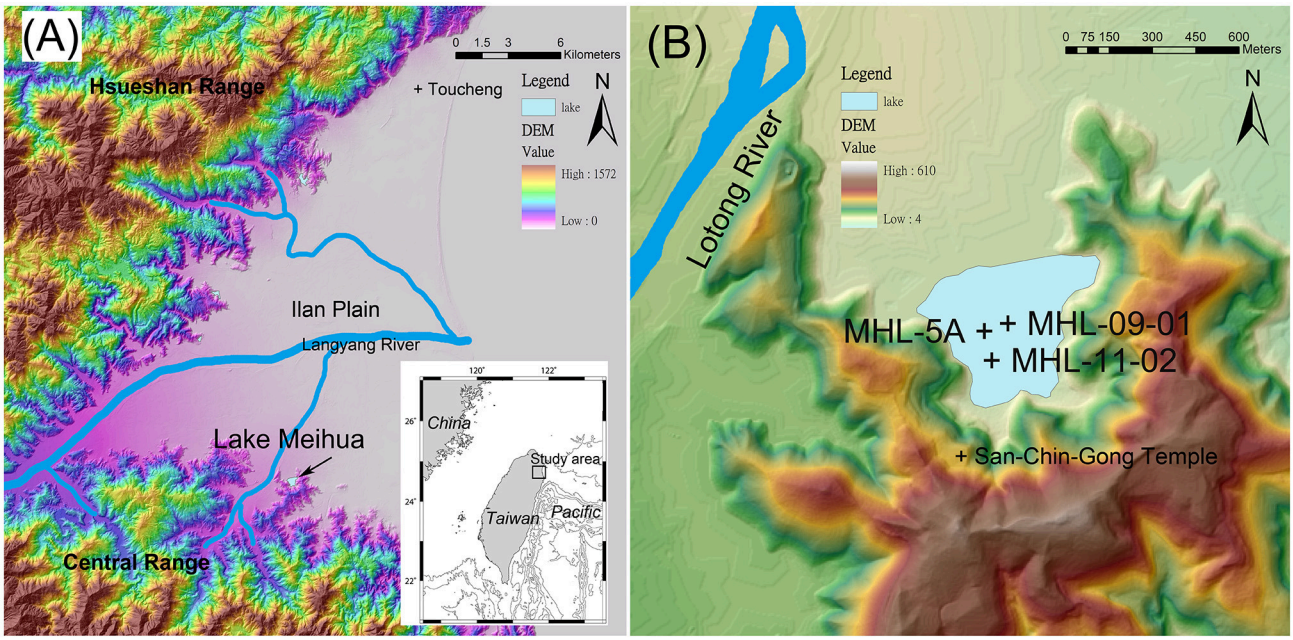

FIGURE 1 | (A) Digital elevation model (DEM) of the Ilan Plain showing the location of the Lake Meihua. The inset map shows the location of Ilan Plain in northeastern Taiwan. **(B)** Locations of the sediment cores investigated in this study, the topographic map is based on 40 m DEM.

although the dominating component of the vegetation is strongly influenced by topography and altitude (Su, 1984). The vegetation of the surrounding mountains consists of subtropical to warm temperate forests dominated by Lauro-Fagaceae elements common in the *Castanopsis-Machilus* Zone (Chen, 2000). Today, much of the plain is cultivated (mostly rice), or covered by herbaceous plants and cultivated trees (Lin et al., 2007).

Human Activities

The history of human settlement in northeastern Taiwan has been reconstructed from archaeological remains (Liu, 1995; Chen et al., 2007b) and historical documents (Yao, 1829; Lu, 1970; Knapp, 1976; Bai, 1991). The colonization history of the Ilan area can be traced back to Neolithic (∼5000 yr BP) and Iron age (∼1300 yr BP) settlements by aboriginal people of Taiwan (Liu, 1995; Chen et al., 2007b). Before the seventeenth century, Taiwan was primarily populated by aboriginal groups and only a limited number of Chinese migrants due to the isolation policy of the Chinese government (Lu, 1970). However, in the early seventeenth century Chinese settlers mainly from southeastern China started to migrate to Taiwan because of the civil war between the Ming and Qing (or Ching) dynasties on mainland China (Knapp, 1976). Moreover, during the two centuries after the Qing dynasty annexed Taiwan in AD 1683, Chinese settlers established agricultural villages from west to east across the island. Therefore, the settlement history of northeastern Taiwan began quite late compared to western and southern Taiwan due to its isolated geographical location (Lu, 1970; Bai, 1991).

The town of Ilan was first recorded as Kibanuran and occupied by an aboriginal people named Kavalan (meaning people living on the plain). Chinese settlers reached northern Ilan at ∼AD 1768. After fighting with the aboriginal Kavalan people for several years, a settler named Sha Wu and his group finally began their agriculture practices near Toucheng (northern Ilan, **Figure 1A**) in AD 1796 (Lu, 1970). Along with the continuing development of Ilan Plain, Chinese settlers reached the area near Lake Meihua at ∼AD 1874 and spread to the Suao area (southern Ilan) in the following decades (Lu, 1970; Bai, 1991).

MATERIALS AND METHODS

Lacustrine Core Sampling

The two short lacustrine cores MHL09-01 and MHL11-02 used for this study were collected on October 1st 2009 and March 9th 2011 from Lake Meihua (**Figure 1B**). To obtain high-quality, undisturbed cores, we used 9-cm diameter transparent acrylic tubes with sharp edges which were inserted directly into the lake sediments on the rubber boat. The tops of the tubes were sealed to maintain the air pressure, and the tubes were pulled up directly to get the lake sediments. Since the tubes were transparent, the interface between water and sediment can be clearly seen to make sure the sediments were well preserved. The recovery length for core MHL-09-01 was 76 cm, and 68 cm for core MHL-11-02. After collection, the cores were kept upright and transported to the laboratory for splitting, description, and subsampling. The archive-halves were used for Itrax-XRF core scanner analysis, and the working-halves were subsampled at a resolution of 0.5 to 1 cm for radionuclides, TOC, and TOC/TN analysis, and 1 to 5 cm for grain size analysis. In addition, the top 205 cm of the 28.63 m long core MHL-5A (**Figure 1B**), which was obtained using hydraulic

piston coring in 2005, was used for palynological studies. The sampling intervals for the pollen study were every 10 cm with 1 cm slice thickness, and 2 ml of each slice were used for pollen analysis.

Age Determination

The age models for cores MHL-09-01 and MHL-11-02 were constructed by using excess ^{210}Pb ($^{210}Pb_{ex}$) and were further constrained by the subsurface maximum of ^{137}Cs and ^{239,240}Pu (circa A.D. 1963), which are consistent with the history of nuclear fallout. In brief, ^{210}Pb (via ^{210}Po) and ^{239,240}Pu in core MHL-09-01 were measured by α-spectrometry, and ^{210}Pb in core MHL-11-02 was measured by γ-spectrometry. ^{137}Cs in both cores was measured by γ-spectrometry. ^{209}Po and ^{242}Pu spikes obtained from ORNL (Oak Ridge National Laboratory), calibrated with NIST-certified SRM-4327 and SRM-996 standards, were used as the yield determinants and added before the digestion of the samples. The details of the radiochemical procedures can be found in Huh and Su (1999) and the references therein. After radiochemical procedures, the Po isotopes were plated onto a silver disc at 80–90°C for 1 h, and the Pu isotopes were electroplated onto a stainless steel disc. ^{210}Pb, ^{214}Pb, and ^{137}Cs in MHL-11-02 were measured by γ-spectrometry based on photon energies around 46.52 keV, 351.99 keV, and 661.62 keV, respectively. Three HPGe detectors were engaged in this study to count over a series of sectioned sediment samples, including one GEM-type (ORTEC GEM-150240) with 150% efficiency (relative to 3 × 3 NaI), one GMX-type (ORTEC GMX-120265) with 100–120% efficiency and one LoAX-type (ORTEC LoAX-70450) with 70% efficiency. The counting efficiencies of the three detectors were calibrated by IAEA reference materials 327 and 375 for sample weight at 100 g as a reference, coupled with an in-house secondary standard for various masses (from 20 to 250 g) to calibrate the effect of sample mass on the attenuation of γ-ray of various energies. Sedimentation accumulation rates were determined from depth profiles of $^{210}Pb_{ex}$. The total ^{210}Pb and the fraction of the total ^{210}Pb that is supported by its precursor, ^{226}Ra. Due to the very short half-lives of all intermediate nuclides between ^{226}Ra and ^{210}Pb, the supported ^{210}Pb is generally in secular equilibrium with all its precursors from ^{226}Ra to ^{214}Pb. The activity of $^{210}Pb_{ex}$ was obtained by subtracting the activity of ^{214}Pb from that of the measured (i.e., total) ^{210}Pb ($^{210}Pb_{ex} = {}^{210}Pb - {}^{214}Pb$). In theory, the activity of $^{210}Pb_{ex}$ is the highest at the core top and decreases down-core because of radioactive decay. Under the assumption of a constant ^{210}Pb flux and a constant sedimentation rate (with the layer of Unit II excluded), the concentration of $^{210}Pb_{ex}$ downcore can be described by:

$$C = C_0 \exp(-\lambda t) \quad (1)$$

where C is $^{210}Pb_{ex}$ at depth Z, C_0 is $^{210}Pb_{ex}$ at the core top (i.e., $Z = 0$), λ is the decay constant of ^{210}Pb (0.0311 yr^{-1}), and t is the post-depositional time. Given that $t = Z/S$, where S indicates sedimentation rate, previous equation can be transformed to

$$C = C_0 \exp[(-\frac{\lambda}{S})Z] \quad (2)$$

Therefore, we expect to see straight regression lines by plotting C vs. Z on semi-log plots, which have slopes equal to $-\lambda/S$. From the slopes, the sedimentation rate (S) can be determined. The details about the γ-spectrometry method, including the standard materials used to calibrate the detectors and QA/QC of the data, can be found in previous studies (Huh and Su, 1999; Su and Huh, 2002; Huh et al., 2011).

The age model for the uppermost sediments of core MHL-5A is based on the linear interpolation between the date of coring at top, and one AMS (Accelerator Mass Spectrometry) ^{14}C analysis from wood fragments at 194 cm performed by the Rafter Radiocarbon Laboratory, Institute of Geological and Nuclear Sciences, New Zealand. The ^{14}C date was then calibrated using CALIB 7.1.0. (http://calib.qub.ac.uk/calib/). All following ages are given as calibrated years AD.

Multiproxy Sediment Core Analyses

Continuous downcore measurements of elemental variations were done at the Itrax-XRF Core Scanner Lab, Department of Geosciences, National Taiwan University (NTU). Archive halves of core MHL-09-01 and MHL-11-02 were analyzed using the 3 kW Mo target. The XRF measurements were analyzed at 30 kV, 44 mA, 2 mm resolution with 5 s exposure time for MHL-09-01, and 30 kV, 29 mA, 200 μm resolution with 15 s exposure time for MHL-11-02. The original XRF spectrums were processed by the Q-Spec software provided by Cox Analytical Systems to obtain element peak areas as counts. Beside the element counts, the ratio of incoherent to coherent scattering (inc/coh) may be used as an estimate of sedimentary organic contents in lacustrine sediments. In theory, the inc/coh scattering is higher for elements with a low atomic mass than for elements with higher atomic mass (Hodoroaba and Rackwitz, 2014), and therefore has been linked to the mean atomic number and can be largely related to the content of organic matter (Guyard et al., 2007; Rolland et al., 2008; Sáez et al., 2009; Brunschön et al., 2010). Therefore, the inc/coh can become an important reference for the strategy of further sampling, and thus to reduce the measure time and costs on organic experiments. Moreover, optical and radiographic images of the cores were also obtained by the same device.

Samples for total organic carbon (TOC) and total nitrogen (TN) were analyzed at the Department of Earth and Life Science, University of Taipei, following the procedures described in Yang et al. (2011b). In brief, each freeze-dried sample was pre-treated with 1 N HCl to remove carbonate, then washed with deionized water and dried in an oven at 60°C. The samples were then wrapped in a tin capsule and combusted using a ThermoQuest EA1110 elemental analyzer to measure the TOC and TN, and thus the atomic ratio of TOC/TN. The precision of the measurements for TOC and TN is ± 0.4 wt. % and ± 0.6 wt. %, respectively.

Samples for grain size analysis were analyzed at the Institute of Oceanography, National Taiwan University. 1 g of wet sediment was treated sequentially with 10 ml of 15% H_2O_2 and 7.5 ml of 10% HCl to remove organic materials and carbonates, and washed with deionized water. Prior to the analysis, 10 ml of 1% $Na(PO_3)_6$ was added to each sample followed by vigorous shaking. The samples were then ready for analysis

using a Beckman Coulter LS-13 320 Laser diffraction particle size analyzer. Reproducibility of replicate analyses of sample and working standard were better than 95%.

For the palynological study, the sample preparation of core MHL-5A followed the classic procedures outlined by Moore et al. (1991), and slightly modified by Lin et al. (2007), involving treatments with hydrochloric acid, potassium hydroxide, sodium pyrophosphate, hydrofluoric acid and acetolysis. For each sample, more than 200 non-aquatic pollen grains were counted, except for samples with very low pollen counts. The taxonomic nomenclature in the pollen diagrams followed the published keys from Huang (1981), Chen and Wang (1999), and the references therein. Percentage calculations and construction of the diagrams were performed using the Tilia and TGView programs (provided by Dr. Eric Grimm, Illinois State Museum). In this study, we will only use the palynological data of the uppermost 205 cm from core MHL-5A.

RESULTS

Lithology

Using sedimentological core descriptions, grain size analysis, and observations of radiographic images, five sedimentary units were defined and correlated between MHL-09-01 and MHL-11-02 (**Figure 2**, **Table 1**). From bottom to top, Unit V (58–76 cm in MHL-09-01 and 66–68 cm in MHL-11-02) consists of a laminated light gray-yellowish silt with gradual changes at the upper boundary. Unit IV (34–58 cm in MHL-09-01 and 34–66 cm in MHL-11-02) is a laminated light gray silt with gradual upper boundary. Unit III (17–34 cm in MHL-09-01 and 18–34 cm in MHL-11-02) is a soupy dark gray silt to very-fine-sand and has a sharp upper boundary especially in MHL-09-01. Unit II (10.5–17 cm in MHL-09-01 and 9–18 cm in MHL-11-02) is made up of a massive yellowish silt with gradual upper boundary, followed by Unit I (0–10.5 cm in MHL-09-01 and 0–9 cm in MHL-11-02), which is a homogenous dark gray silt. In this study, we will focus at Unit III to I. For more details on the lower units, please refer to Huang (2011).

Chronology

Activities of all measured fallout nuclides show anomalously low values in Unit II for both cores (**Figure 2**). However, the $^{210}Pb_{ex}$ profiles of the segments above and below Unit II both show the expected exponential decreases with depths, allowing the sedimentation accumulation rates based on $^{210}Pb_{ex}$ to be estimated. Further chronological constraint comes from the profiles of ^{137}Cs which are characterized by a pronounced peak at the 18.0–18.5 cm interval in MHL-09-01 (also $^{239,240}Pu$ peak) and 17.0–17.5 cm in MHL-11-02, reflecting the history of atmospheric nuclear weapons testing which showed a global fallout maximum in AD 1963 (Pennington et al., 1973).

In MHL-09-01, since the Unit II is covered by 10.5 cm of sediment at the top and commenced ~1.5 cm above the global

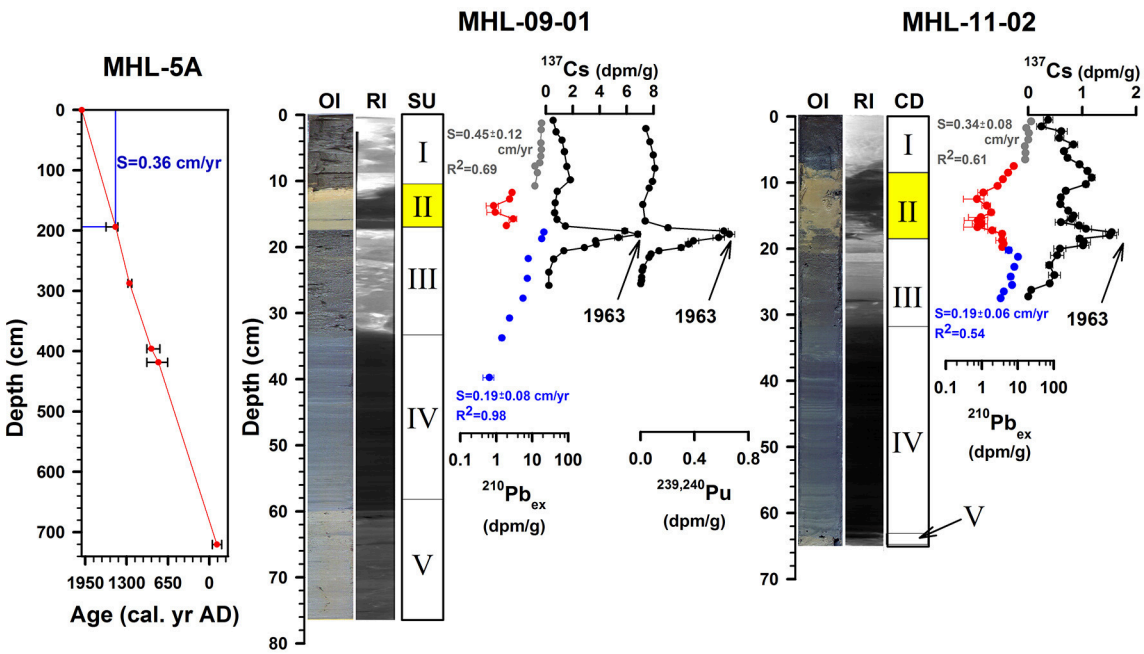

FIGURE 2 | The depth vs. radiocarbon age profile of the upper 720 cm in MHL-5A, and the lithologies and chronologies for core MHL-09-01 and MHL-11-02. The blue box in the left panel shows the segment that was used for palynological reconstruction. This interval has a mean sedimentation rate of 0.36 cm yr^{-1}, which is close both to the average of the age model in MHL-5A, and in agreement with the sedimentation rates reconstructed for the two shorter cores. OI: optical image obtained by Itrax-XRF core scanner; RI: radiographic image obtained by Itrax-XRF core scanner; SU: Sedimentary units. The chronologies are based on the radionuclide profiles of $^{210}Pb_{ex}$, ^{137}Cs and, $^{239,240}Pu$ in core MHL-09-01 and $^{210}Pb_{ex}$ and ^{137}Cs in MHL-11-02. The ^{210}Pb-based sedimentation rates above (in gray color) and below unit II (in blue color) in both cores are also shown next to the $^{210}Pb_{ex}$ profiles.

TABLE 1 | Sedimentary units, its characteristic features and inferred depositional conditions of the Lake Meihua sedimentary sequence in core MHL-09-01 and MHL-11-02.

Sedimentary units	Sedimentological features	Inferred depositional conditions
I	Massive dark gray silt	Modern condition of the lake
II	Massive yellowish silt	Construction Event by San-Chin-Gong Temple
III	Soupy dark gray silt to very fine sand (small plant debris less than 0.2 mm has been found in MHL-11-02)	Impact of Chinese settlers
IV	Laminated light gray silt	Average condition of the lake
V	Laminated light gray-yellowish silt	Impact of flood event (Huang, 2011)

fallout maximum (circa AD 1963), the age of the Unit II can be constrained by ^{210}Pb chronology (**Figure 2**). By least-square fitting of the $^{210}Pb_{ex}$ data above and below Unit II, we obtained ^{210}Pb-based sedimentation accumulation rates of 0.45 ± 0.12 cm yr^{-1} ($R^2 = 0.69$, $n = 10$) and 0.19 ± 0.08 cm yr^{-1} ($R^2 = 0.98$, $n = 9$), respectively. Thus, the 6.5 cm thick Unit II was deposited ∼7 years after the fallout maximum and ∼24 years before the core was collected. In other words, Unit II accumulated during AD 1970–1985, with a mean sedimentation accumulation rate of ∼0.40 cm/yr. Also, the pattern of radionuclide profiles in MHL-11-02 is similar to those in MHL-09-01 (**Figure 2**). The ^{210}Pb-based sedimentation accumulation rates above and below Unit II are 0.34 ± 0.08 cm yr^{-1} ($R^2 = 0.61$, $n = 7$) and 0.19 ± 0.06 cm yr^{-1} ($R^2 = 0.54$, $n = 8$), while the sedimentation accumulation rate in Unit II is ∼0.37 cm yr^{-1}. Therefore, the ages of Unit II in both cores are perfectly consistent with the construction period of San-Ching Gong Temple near the lake (see discussion).

The chronology in the upper 205 cm of MHL-5A is based on the linear interpolation between coring date (i.e., AD 2005) and 1 AMS ^{14}C dating at 194 cm (wood fragments, the dating result is 400 ± 30 yr BP and the median calibrated age is 1476 in the 2σ range of AD 1437–1624, **Table 2**), resulting in a mean sedimentation rate of ∼0.36 cm yr^{-1}. The general sedimentation rate indicated by these two age control points is supported by deeper radiocarbon dates in MHL-5A, and also similar to the sedimentation rates that were estimated for the two shorter cores in this study (**Figure 2**, **Table 2**), as well as by previous studies (Huang, 2011; Chen et al., 2012).

Multiproxy Sediment Core Analyses

XRF Core Scanning Measurements

The downcore profiles of inc/coh and Ti in core MHL-09-01 and MHL-11-02 obtained by the Itrax-XRF core scanner will be discussed in this study. The upper 12 cm of XRF measurements in core MHL-09-01 had to be removed because of cracks that formed due to drying during storage. Generally, the inc/coh stays low in lowermost Unit V and IV, increased gradually in Unit III, continuing with an abrupt drop in Unit II and then returning to high values in Unit I. Ti shows an opposite pattern, remaining high in Unit V and IV, decreasing gradually in Unit III, continuing with an abrupt rise in Unit II and then returning to low values. The relationship between inc/coh and the organic contents is also further confirmed by the positive correlation between inc/coh and TOC measurements (see below) in this study (correlation coefficient, $r = 0.90$ in MHL-09-01 and 0.88 in MHL-11-02) (**Figure 3**).

The inc/coh and Ti profiles in both cores show a strong negative correlation (correlation coefficient, $r = -0.90$ in MHL-09-01 and -0.94 in MHL-11-02) (**Figure 3**). These negative correlations are attributed to the well-known closed-sum effect caused by the dilution of organic materials (Calvert, 1983; Rollinson, 1993). Consequently, the measured variations in the elements (i.e., Ti) will to a large extent mirror the changes in the organic materials (i.e., inc/coh). Some studies have suggested to normalize the elements in the lithogenic component of the sediment against a conservative element (e.g., Al) to allow changes in the input of the elements to be addressed (Kylander et al., 2011; Löwemark et al., 2011). However, it is difficult to remove all the influences generated by variations in organic components (Huang, 2011). Therefore, the interpretation of elemental variations from XRF scanning must be treated with caution especially in organic rich lacustrine sediments, and only element data for Ti is included in this study.

Organic Geochemistry

The general trends of TOC and atomic TOC/TN are similar in both cores (**Figure 3**), while the difference of maximum values may be attributed to the core locations in the lake. The organic content of sediments in Lake Meihua is highly variable, ranging from 0.5% to ∼8.0% for TOC (**Figure 3**). Lower values less than 2.0% occur in Units V and IV. A rising trend from the base of Unit III (from 0.5% to ∼8.0% in MHL-09-01 and ∼0.3% to ∼4.0% in MHL-11-02), continues with an abrupt drop to 1.0% in Unit II and then returns to ∼4.0% in Unit I of both cores.

The TOC/TN profiles show parallel changes to the TOC (especially in MHL-11-02, **Figure 3**), but vary from 4.0 to 6.5 in MHL-09-01 and 4.0 to 10.0 in MHL-11-02. Lower values occur in Units V and IV, followed by a rising trend up to 5.0 in MHL-09-01 and up to 9.0 in MHL-11-02 in Unit III. An abrupt drop of TOC/TN was found in Unit II, followed by increasing values in Unit I.

Grain Size Analysis

The results of mean grain size analysis are similar in both MHL-09-01 and MHL-11-02 (**Figure 3**). Both cores show finer grain sizes in Unit V, VI, II, and I, ranging from fine-silt to very-fine-silt (Φ:6.0–7.5), while a coarsening upward trend was found in both cores in Unit III. This unit coarsens from silt to very-fine-sand (Φ:6.0–3.2), with the highest peaks at the boundary between Unit III and Unit II. In MHL-11-02, although the highest peak seems to be 3.5 cm below the Unit III/II boundary. This discrepancy is likely caused by mixing or deformation during coring, as can be clearly seen on the optical and radiographic images (**Figure 2**).

TABLE 2 | Radiocarbon dates and corresponding calibrated ages of the upper 720 cm in core MHL-5A from the Lake Meihua.

Depth (cm)	^{14}C age (yr BP)	2σ cal. range (cal. yr AD)	Median Probability (cal. yr AD)	Laboratory code
194 ± 1	400 ± 30	1437–1624	1476	NZA-27808
287.5 ± 0.5	767 ± 30	1218–1282	1255	NZA-27860
396 ± 1	1139 ± 30	777–982	912	NZA-25241
418.5 ± 0.5	1230 ± 90	654–982	800	NTU-4527
720.5 ± 0.5	2098 ± 30	(−194)–(−47)	−121	NZA-25269

All the dating materials are from wood fragments

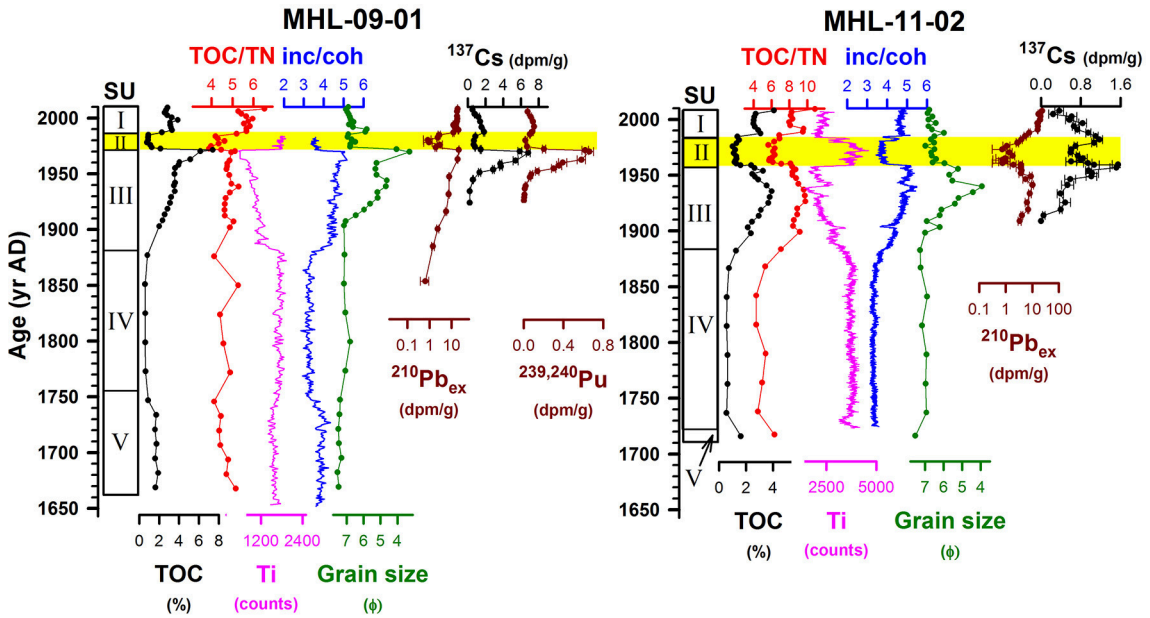

FIGURE 3 | Sediment geochemical records of core MHL-09-01 and MHL-11-02. SU (Sedimentary units), TOC (%, total organic carbon), TOC/TN, inc/coh (organic indicator obtained by Itrax-XRF core scanner), grain size and radionuclides are shown. The interval highlighted by the yellow bars can be related to the erosion caused by the construction of a San-Chin-Gong Temple complex on the hillslope south of the lake from AD 1970 to 1982. The increase in organic matter in Unit III likely represents the land development by Chinese settlers in the late 19th century.

Pollen Assemblages

Pollen of more than 100 taxa, including either families or genera, were identified from the uppermost 205 cm of core MHL-5A. The studied interval represents the time period since AD 1440 and the major pollen taxa can be divided into two zones, as shown in **Figure 5**.

Zone PZ2 (205–55 cm; AD 1476–1860).

This zone is characterized by stable levels of abundant tree and shrub pollen, accounting for over 60% of the terrestrial pollen sum. *Cyclobalanopsis*, *Quercus*, *Alnus*, *Lagerstroemia*, and *Liquidambar* are the predominant contributors, accompanied by *Bischofia*, *Myrica*, *Ardisia*, *Glochidion*, and *Helicia*. The percentages of herbs and ferns are low.

Zone PZ1 (55–0 cm; AD 1860–present).

This zone is marked by a sharp decline in tree pollen, and a large increase in herbaceous and fern pollen. *Lagerstroemia* and *Liquidambar* show dramatic declines, while *Ardisia*, *Engelhardia*, *Elaeocarpus*, *Bischofia*, *Schefflera*, and *Calamus* also decrease. Secondary forest taxa, such as *Alnus, Mallotus, Trema* become significant. Herbs, such as Poaceae, Cyperaceae, *Artemisia*, Apiaceae, Amaranthaceae, and Asteraceae rise conspicuously.

DISCUSSION

The Sources of Sediments to Lake Meihua

The TOC/TN can be used to identify the sources of organic materials in sediments as either autochthonous or allochthonous (Meyers, 1994; Lamb et al., 2006; Yang et al., 2011a, 2014). As documented by Meyers (1994) and Lamb et al. (2006), the TOC/TN is usually less than 9 for lacustrine algae (representing the autochthonous primary source) and higher than 12 for vascular plants (representing the allochthonous primary source), respectively. In the Lanyang River catchment, the TOC/TN of primary materials, such as bedrocks, river sediments and soils have been investigated by Kao and Liu (2000) (**Figure 4**), and

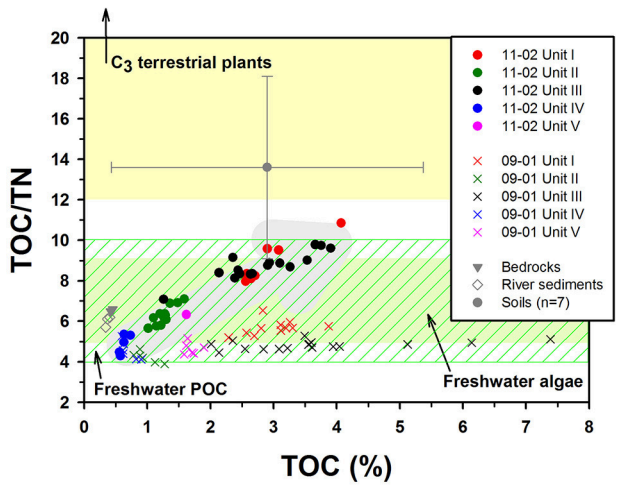

FIGURE 4 | Plot of TOC (%) against TOC/TN, indicating the potential sources of sediments of the Lake Meihua. Units I to V from cores MHL-09-01 and MHL-11-02 are shown. The bedrock (gray triangle), river sediments (gray diamond) and soil data (gray circle with error bar, $n = 7$) are from Kao and Liu (2000) in the Lanyang River catchment, while the TOC/TN ranges of freshwater algae, freshwater particulate organic carbon (fresh water POC) and C_3 terrestrial plants are from Lamb et al. (2006).

also been used to identify the organic sources of lacustrine sediments as reported by Yang et al. (2014) and Yang et al. (2011a).

As suggested by the MHL-5A record in Huang (2011), the TOC and TOC/TN values in Unit IV of both MHL-09-01 and MHL-11-02 (**Figure 4**, blue circle and blue cross) can represent the long-term average conditions in Lake Meihua during the past millennium. The increasing trends of TOC/TN and TOC from Unit IV to Unit III of MHL-11-02 in **Figure 4** (gray arrow) likely indicate an increasing input of carbon-rich terrestrial organic materials in both Unit III and Unit I. However, the bedrocks and river sediments cannot be the major components of these increasing signals because of their low TOC contents (∼0.5%, **Figure 4**). Therefore, the soils and the plant debris (found in Unit III of MHL-11-02, **Table 1**) seem to be the main contributors of the increasing organic signals. Conversely, the abrupt drop in Unit II represents the strong dilution by minerogenic materials, indicated also by its low values of TOC, TOC/TN, and radionuclides.

However, the increasing trend of TOC/TN in MHL-09-01 is insignificant (**Figures 3**, **4**), although the maximum values of TOC are actually two times higher than those in MHL-11-02. Such observation may be explained as the distance effects of the coring locations in the lake. The terrestrial organic material from the catchment may settle down before it reaches to the center of the lake, where MHL-09-01 was collected. Furthermore, since the TOC/TN in MHL-09-01 remains in the range of freshwater algae, the higher TOC in MHL-09-01 can simply be explained as the lacustrine algae blooming associated with the terrestrial inputs.

The Impact from Construction of San-Chin-Gong Temple

The yellowish Unit II in both cores is the most characteristic unit in the cores. However, the lower values of inc/coh, TOC, TOC/TN, radionuclides in Unit II are very different from the flood layers reported in previous study in Lake Meihua (Huang, 2011; also in the Unit V of this study). There are 8 layers with higher values of inc/coh, TOC, TOC/TN, and grain size in the last 1200 years, and they have been explained as the overbank flooding events and can be linked to the regional climate and earthquake signals (Huang, 2011). Therefore, the natural mechanism cannot explain the presents of Unit II.

The most conspicuous sign of human activities around Lake Meihua is the large temple complex called San-Chin-Gong Temple (**Figure 6**) which is sitting on the slope to the south of the lake (**Figure 1B**). As the headquarters of the Taoism Association in Taiwan, the main building of the temple was constructed over an area of 4 ha during AD 1970–1982, followed by the addition of several annexes in the ensuing years. Such a massive construction in a relatively small catchment must have had a great impact on local environment and the lake just beneath the hill.

The age models for the yellowish Unit II in both cores (**Table 1**, **Figures 2**, **3**) are perfectly linked with the historical temple-building record (**Figure 3**). The radionuclide age at the upper boundary of Unit II in MHL-09-01 is AD 1985 (derived from the upper $^{210}Pb_{ex}$ sedimentation rate and the coring date), while the age at the lower boundary is AD 1970 (derived from the ^{137}Cs peak in AD 1963 and the lower $^{210}Pb_{ex}$ sedimentation rate). Thus, the age of Unit II perfectly match with the documented record of temple construction from AD 1970–1982.

The peaks of TOC, inc/coh and grain size at the boundary of Unit III and II also mark the initial stage of the temple building phase, especially in MHL-09-01. The intense deforestation and excavation for the foundation of the temple and surrounding road systems likely is responsible for these changes. Also, Unit II is characterized by relatively lower values of inc/coh, TOC, TOC/TN, radionuclides, and its yellowish color (**Figures 2**, **3**). These properties reflect the dilution of organic matter and radionuclides content by increased minerogenic material inputs. The enhanced erosion of the exposed hillslope caused by land development activities introduced radionuclides, organic carbon depleted regolith, and/or even the materials that were used in the temple construction into the lake. These anthropogenic influences are further supported by the increased sediment rates in Unit II (0.40 cm yr^{-1} in MHL-09-01 and 0.37 cm yr^{-1} in MHL-11-02). Therefore, the presence of the yellowish Unit II represents the sedimentary evidence for the construction of the temple complex and surrounding road systems. These observations suggest that locally, human induced changes to the erosional pattern may temporally overshadow the natural signals.

After the construction event of the San-Chin-Gong Temple, the intensity of human activities has remained high in the study area. The construction of a dyke and a new sightseeing area around the lake in recent decades likely have caused the increase in sedimentation rates encountered in Unit I (**Figure 2**, 0.45 cm yr^{-1} in MHL-09-01 and 0.34 cm yr^{-1} in MHL-11-02). Also, the return to high levels of inc/coh, TOC and TOC/TN in

Unit I (**Figures 3**, **4**) suggest that runoff delivered more terrestrial organic materials into the lake related to the continuous farming and deforestation in the surrounding area.

Land Development by Chinese Settlers in the Late 19th Century

In the older part of the record, human influence is less dramatic, but still clearly visible from both sedimentary parameters and pollen data. Up till the end of the eighteenth century, the area surrounding Lake Meihua experienced relatively little perturbations from human activities. It was not until AD 1796 that the Chinese settler Sha Wu and his group defeated the aboriginal Kavalan people and invaded the Toucheng area (northeastern Ilan, **Figure 1A**) to extend the frontiers of Chinese settlement and agricultural practices. After that, Chinese settlers started to develop the Ilan Plain, although they were constantly in conflict with the original aboriginal population while extending their territory further, reaching Suao at the southeastern tip of the Ilan Plain in the late nineteenth century (Yao, 1829; Lu, 1970).

The records from Lake Meihua in southern Ilan clearly reflect this history. This study reveals how the increasing trends of inc/coh, TOC, TOC/TN, and grain size in Unit III of both MHL cores (**Figures 3**, **4**) record the agronomic activities of Chinese settlers starting from the late nineteenth century. Historical documents suggest that a Chinese settler named Hui-Huang Chen and his group of people started the cultivation works to the south of Lanyang River in AD 1874 (Bai, 1991), at a site close to Lake Meihua. The deforestation, land clearance and following agricultural practices by Chinese settlers likely caused intensified remobilization of terrestrial material, thereby not only increasing the input of TOC and coarser materials into the lake, but also causing algae booming due to the input of nutrients. These changes in input are also reflected by an increase in plant debris of MHL-11-02, and the less dense nature of the sediments shown in the radiographic images of both cores (**Table 1**, **Figure 2**).

The change in land use is further supported by the palynological data from core MHL-5A (**Figure 5**, PZ1). The dramatic drop in tree and shrub pollen can be attributed to deforestation, while the dominance of herbs and pioneer species, such as *Alnus, Mallotus,* and *Trema* since around AD 1860 (**Figure 5**, PZ1) likely is the result of anthropogenic vegetation changes due to land clearance, and can therefore be linked to the increasing organic content in the Unit III (**Figure 3**). In the present age model of core MHL-5A, the age for the lower boundary of pollen zone PZ1 is situated at about AD 1860 (**Figure 5**). This is just one decade earlier than the change in agriculture activities indicated by the historical record (Bai, 1991) and the radionuclides ages in the beginning of Unit III in both short cores. However, the low resolution sampling for radiocarbon dating in core MHL-5A makes the exact age of the shift in pollen assemblages uncertain. The sedimentation rates obtained by $^{210}Pb_{ex}$ together with the radionuclides fall out maximum in AD 1963 obtained by ^{137}Cs and $^{239,240}Pu$ in MHL-09-01 and MHL-11-02 suggested that the lower boundary of Unit III can be dated to the 1880s (**Figure 3**). Thus, the evidence of anthropogenic impacts in the lacustrine cores from Lake Meihua may certainly be linked to the agricultural practices by Chinese settlers since AD ~1874, as recorded in historical documents (Bai, 1991).

In contrast to Lake Meihua, where anthropogenic influence can only be clearly detected for the last few 100 years or so, palynological records from Lake Dahu in northern Ilan show a human influence at least since around AD 1400.

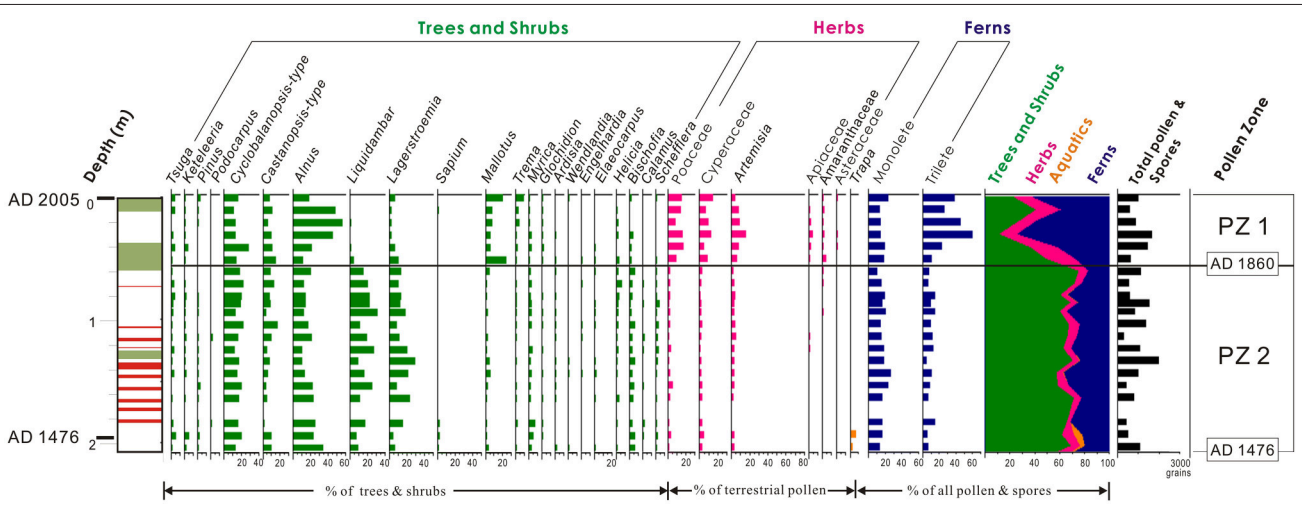

FIGURE 5 | Pollen percentage diagram of selected taxa from core MHL-5A. Pollen percentage diagram of selected taxa from core MHL-5A in the Lake Meihua. In the pollen zone-PZ1, the increasing trends of *Alnus*, *Mallotus*, *Trema* and herbs coupled with the increasing trends of organic proxies in Unit III of **Figure 3** suggest that the neighboring area has been significantly affected by agronomic activities starting around AD 1880s and may be attributed to the arrival of Chinese settlers around AD 1874.

FIGURE 6 | View of San-Chin-Gong Temple took from the location of MHL-11-02. As the headquarter of the Taoism Association in Taiwan, the main building of the temple was constructed during AD 1970–1982, followed by the addition of several annexes in the ensuing years.

This suggests that on the northern Ilan Plain, intensive land clearance took place 200 years prior to the arrival of the Chinese settlers (Yang et al., 2014). Consequently, the great drop in arboreal pollen concentration around AD 1400 in Lake Dahu can be attributed to deforestation by aboriginal people to clear land for agriculture. According to the archaeological studies on Ilan Plain (Liu, 1995), the almost 500 years earlier development history in Lake Dahu compared to Lake Meihua can be attributed to the distribution of aboriginal people on Ilan Plain and the later arrival of Chinese settlers in southern Ilan.

This study suggests that while modest land clearance may result in an increase in TOC due to enhanced erosion of the topsoil, a massive intervention, however, such as the temple construction may actually result in a drop in TOC due to dilution of the organic input by massive influx of lithogenic material from the exposed regolith. Where the local end-members of the organic sources are known, TOC/TN can be used to identify the sources and possible transport mechanisms of sediments.

CONCLUSION

Based on sedimentological and geochemical natural archives from Lake Meihua on the Ilan Plain, several general conclusions regarding the interactions between humans and the environment, and how these interactions are documented in the sedimentary record, may be drawn:

- The presence of a yellowish layer with lower levels of inc/coh, TOC, TOC/TN, and radionuclides can be tied to intensified erosion caused by the land development associated with the construction of the San-Chin-Gong Temple during AD 1970–1982.
- During the temple construction phase, the signals in the sedimentary archives were completely dominated by this event, demonstrating how anthropogenic processes can locally overshadow natural processes in the archives.
- Changes in land use, land clearing, and agriculture are reflected both in sedimentary parameters, such as the TOC, inc/coh, TOC/TN, and grain size, and in pollen counts. The arrival of Chinese settlers, and the following agriculture activities on the southern Ilan Plain, thus can be detected in the sedimentary record since ∼AD 1874.

This study demonstrates how lacustrine sediments can be used as recorders of human activities in agreement with historical documents. However, due to the complexity of lake systems in catchments with steep topographies and high erosion rates, a multiproxy approach is necessary to disentangle the relative influence of the different processes.

AUTHOR CONTRIBUTIONS

JH: design of the work, sample taking, geochemical analysis, and drafting the article. CH, WL, and CS: design of the work, sample taking, radionuclide and grain size analysis and interpretation, and drafting the article. KW, LL, SS, and TL: design of the work, funding provider, and drafting the article. SL: Pollen sample analysis and interpretation, and drafting the article. TY, ML: design of the work, sample taking, organic sample analysis and interpretation, and drafting the article.

ACKNOWLEDGMENTS

We are grateful to Miss Yun-Chun Wang, Queenie Chang and Emma Tung for assistance during sample processing and manuscript preparation. Funding for this research was provided by the research project "Environmental Change and Human Activity over the Last 1000 Years in the Lang-Yang River Drainage System: ECHA1000" (NSC 98-2627-M-002-010).

REFERENCES

Bai, Z. C. (1991). "The critical biographies of Chinese settler Hui-Huang Chen (in Chinese)," in *Taiwan Historica,* ed Academia Historica of Taiwan (Taipei: Academia Historica of Taiwan Press), 215–232.

Brunschön, C., Haberzettl, T., and Behling, H. (2010). High-resolution studies on vegetation succession, hydrological variations, anthropogenic impact and genesis of a subrecent lake in southern Ecuador. *Veg. Hist. Archaeobot.* 19, 191–206. doi: 10.1007/s00334-010-0236-4

Calvert, S. E. (1983). Geochemistry of pleistocene sapropels and associated sediments from the eastern Mediterranean. *Oceanol. Acta* 6, 255–267.

Chen, C. W., Kao, C. M., Chen, C. F., and Dong, C. D. (2007a). Distribution and accumulation of heavy metals in the sediments of Kaohsiung Harbor, Taiwan. *Chemosphere* 66, 1431–1440. doi: 10.1016/j.chemosphere.2006.09.030

Chen, H. F., Wen, S. Y., Song, S. R., Yang, T. N., Lee, T. Q., Lin, S. F., et al. (2012). Strengthening of paleo-typhoon and autumn rainfall in Taiwan corresponding

to the Southern Oscillation at late Holocene. *J. Quaternary Sci.* 27, 964–972. doi: 10.1002/jqs.2590

Chen, S. H., and Wang, Y. F. (1999). Pollen flora of Yuenyang Lake Nature Preserve, Taiwan (I). *Taiwania* 44, 82–136.

Chen, T. (2000). "Plant ecology of lowland areas in northern Taiwan (in Chinese)," in *Botanical Garden Resources and Its Management*, ed H. Yen. (Taichung: National Museum of Natural Science Press), 9–33.

Chen, W. S., Yang, C. C., and Yang, H. C. (2009). "How to reconstruct the depositional framework of the late Quaternary subsurface sedimentary sequence in the Taiwan coastal plains? (in Chinese)," in *Special Publication of the Central Geological Survey 22*, ed Central Geological Survey (Taipei, Taiwan: Central Geological Survey), 101–114.

Chen, Y. B., Chiu, S. J., and Li, Z. Y. (2007b). *Report of Salvage Excavation on the Site Kiwulan, Ilan County (in Chinese)*. Ilan: Lanyang Museum Press.

Croudace, I. W., Rindby, A., and Rothwell, R. G. (2006). "ITRAX: description and evaluation of a new multi-function X-ray core scanner," in *New Techniques in Sediment Core Analysis,* ed. R. G. Rothwell (London: The Geological Society of London), 51–63.

Dadson, S. J., Hovius, N., Chen, H. G., Dade, W. B., Hsieh, M. L., Willett, S. D., et al. (2003). Links between erosion, runoff variability and seismicity in the Taiwan orogen. *Nature* 426, 648–651. doi: 10.1038/nature02150

Guyard, H., Chapron, E., St-Onge, G., Anselmetti, F. S., Arnaud, F., Magand, O., et al. (2007). High-altitude varve records of abrupt environmental changes and mining activity over the last 4000 years in the Western French Alps (Lake Bramant, Grandes Rousses Massif). *Quaternary Sci. Rev.* 26, 2644–2660. doi: 10.1016/j.quascirev.2007.07.007

Ho, C. S. (1986). *An Introduction to the Geology of Taiwan (in Chinese)*. Taipei: The Ministry of Economic Affairs.

Hodoroaba, V. D., and Rackwitz, V. (2014). Gaining improved chemical composition by exploitation of Compton-to-Rayleigh intensity ratio in XRF analysis. *Anal. Chem.* 86, 6858–6864. doi: 10.1021/ac5000619

Huang, C. Y. (1981). *Spore Flora of Taiwan*. Taipei: Botany Department National Taiwan University.

Huang, J. J. (2011). *Linkage between Natural Disasters and Kiwulan Cultural Hiatus Over the Last 1000 Years in the Lanyang Drainage System (in Chinese)*. Master's thesis. Taipei: National Taiwan University.

Huang, J. J., Löwemark, L., Chang, Q., Lin, T. Y., Chen, H. F., Song, S. R., et al. (2016). Choosing optimal exposure times for XRF core-scanning: suggestions based on the analysis of geological reference materials. *Geochem. Geophys. Geosyst.* 17, 1558–1566. doi: 10.1002/2016gc006256

Huang, K. M., and Lin, S. (2003). Consequences and implication of heavy metal spatial variations in sediments of the Keelung River drainage basin, Taiwan. *Chemosphere* 53, 1113–1121. doi: 10.1016/S0045-6535(03)00592-7

Huh, C. A., Chen, W., Hsu, F. H., Su, C. C., Chiu, J. K., Lin, S., et al. (2011). Modern (<100 years) sedimentation in the Taiwan Strait: rates and source-to-sink pathways elucidated from radionuclides and particle size distribution. *Cont. Shelf Res.* 31, 47–63. doi: 10.1016/j.csr.2010.11.002

Huh, C. A., and Su, C. C. (1999). Sedimentation dynamics in the East China Sea elucidated from ^{210}Pb, ^{137}Cs and ^{239,240}Pu. *Mar. Geol.* 160, 183–196. doi: 10.1016/S0025-3227(99)00020-1

James, L. A. (2013). Legacy sediment: definitions and processes of episodically produced anthropogenic sediment. *Anthropocene* 2, 16–26. doi: 10.1016/j.ancene.2013.04.001

Kao, S. J., and Liu, K. K. (2000). Stable carbon and nitrogen isotope systematics in a human-disturbed watershed (Lanyang-Hsi) in Taiwan and the estimation of biogenic particulate organic carbon and nitrogen fluxes. *Glob. Biogeochem. Cycles* 14, 189–198. doi: 10.1029/1999GB900079

Knapp, R. G. (1976). Chinese frontier settlement in Taiwan. *Ann. Assoc. Am. Geogr.* 66, 43–51. doi: 10.1111/j.1467-8306.1976.tb01071.x

Kylander, M. E., Lind, E. M., Wastegard, S., and Löwemark, L. (2011). Recommendations for using XRF core scanning as a tool in tephrochronology. *Holocene* 22, 371–375. doi: 10.1177/0959683611423688

Lamb, A. L., Wilson, G. P., and Leng, M. J. (2006). A review of coastal palaeoclimate and relative sea-level reconstructions using δ^{13}C and C/N ratios in organic material. *Earth-Sci. Rev.* 75, 29–57. doi: 10.1016/j.earscirev.2005.10.003

Liew, P. M., Wu, M. H., Lee, C. Y., Chang, C. L., and Lee, T. Q. (2014). Recent 4000 years of climatic trends based on pollen records from lakes and a bog in Taiwan. *Quatern. Int.* 349, 105–112. doi: 10.1016/j.quaint.2014.05.018

Lin, S. F., Huang, T. C., Liew, P. M., and Chen, S. H. (2007). A palynological study of environmental changes and their implication for prehistoric settlement in the Ilan Plain, northeastern Taiwan. *Veg. Hist. Archaeobot.* 16, 127–138. doi: 10.1007/s00334-006-0076-4

Liu, Y. C. (1995). "Prehistoric culture type of Ilan region (in Chinese)," in *Proceedings of Ilan Research Symposium,* ed J. Chu (Ilan: Ilan County Government Press), 38–56.

Löwemark, L., Chen, H. F., Yang, T. N., Kylander, M., Yu, E. F., Hsu, Y. W., et al. (2011). Normalizing XRF-scanner data: a cautionary note on the interpretation of high-resolution records from organic-rich lakes. *J. Asian Earth Sci.* 40, 1250–1256. doi: 10.1016/j.jseaes.2010.06.002

Lu, S. X. (1970). *The General History of Ilan County (in Chinese)*. Ilan: Ilan County Government Press.

Meyers, P. A. (1994). Preservation of elemental and isotopic source identification of sedimentary organic matter. *Chem. Geol.* 114, 289–302. doi: 10.1016/0009-2541(94)90059-0

Miller, H., Croudace, I. W., Bull, J. M., Cotterill, C. J., Dix, J. K., and Taylor, R. N. (2014). A 500 year sediment lake record of anthropogenic and natural inputs to Windermere (English Lake District) using double-spike lead isotopes, radiochronology, and sediment microanalysis. *Environ. Sci. Technol.* 48, 7254–7263. doi: 10.1021/es5008998

Montgomery, D. (2007). Soil erosion and agricultural sustainability. *Proc. Natl. Acad. Sci. U.S.A.* 104, 13268–13272. doi: 10.1073/pnas.0611508104

Moore, P. D., Webb, J. A., and Collison, M. E. (1991). *Pollen Analysis*. London: Blackwell Scientific Publications.

Pennington, W., Tutin, T., Cambray, R., and Fisher, E. (1973). Observations on lake sediments using fallout ^{137}Cs as a tracer. *Nature* 242, 324–326. doi: 10.1038/242324a0

Rolland, N., Larocque, I., Francus, P., Pienitz, R., and Laperriere, L. (2008). Holocene climate inferred from biological (Diptera: Chironomidae) analyses in a Southampton Island (Nunavut, Canada) lake. *Holocene* 18, 229–241. doi: 10.1177/0959683607086761

Rollinson, H. R. (1993). *Using Geochemical Data: Evaluation, Presentation, Interpretation*. Upper Saddle River, NJ: Pearson Education.

Sáez, A., Valero-Garcés, B. L., Giralt, S., Moreno, A., Bao, R., Pueyo, J. J., et al. (2009). Glacial to Holocene climate changes in the SE Pacific. The Raraku Lake sedimentary record (Easter Island, 27°S). *Quaternary Sci. Rev.* 28, 2743–2759. doi: 10.1016/j.quascirev.2009.06.018

Shyu, J. B. H., Sieh, K., Chen, Y. G., and Liu, C. S. (2005). Neotectonic architecture of Taiwan and its implications for future large earthquakes. *J. Geophys. Res.* 110:B08402. doi: 10.1029/2004jb003251

Su, C. C., and Huh, C. A. (2002). ^{210}Pb, ^{137}Cs and ^{239,240}Pu in East China Sea sediments: sources, pathways and budgets of sediments and radionuclides. *Mar. Geol.* 183, 163–178. doi: 10.1016/S0025-3227(02)00165-2

Su, H. (1984). Studies on the climate and vegetation types of the natural forests in Taiwan (II): altitudinal vegetation zones in relation to temperature gradient. *Q. J. Chin. Forestry* 17, 57–73.

Syvitski, J., and Kettner, A. (2011). Sediment flux and the Anthropocene. *Philos. Trans. A Math. Phys. Eng. Sci.* 369, 957–975. doi: 10.1098/rsta.2010.0329

Wang, L. C., Wu, J. T., Lee, T. Q., Lee, P. F., and Chen, S. H. (2011). Climate changes inferred from integrated multi-site pollen data in northern Taiwan. *J. Asian Earth Sci.* 40, 1164–1170. doi: 10.1016/j.jseaes.2010.06.003

Wei, K. Y., Chen, Y. G., Chen, W. S., Lai, T. H., Chen, L. C., and Fei, L. Y. (2003). Climate change as the dominant control of the last glacial-Holocene δ^{13}C variations of sedimentary organic carbon in the Lan-Yang Plain, northeastern Taiwan. *West. Pac. Earth Sci.* 3, 57–68.

Yang, T. N., Lee, T. Q., Lee, M. Y., Huh, C. A., Meyers, P. A., Löwemark, L., et al. (2014). Paleohydrological changes in northeastern Taiwan over the past 2 ky inferred from biological proxies in the sediment record of a floodplain lake. *Palaeogeogr. Palaeocl.* 410, 401–411. doi: 10.1016/j.palaeo.2014.06.018

Yang, T. N., Lee, T. Q., Meyers, P. A., Fan, C. W., Chen, R. F., Wei, K. Y., et al. (2011a). The effect of typhoon induced rainfall on settling fluxes of particles and organic carbon in Yuanyang Lake, subtropical Taiwan. *J. Asian Earth Sci.* 40, 1171–1179. doi: 10.1016/j.jseaes.2010.07.016

Yang, T. N., Lee, T. Q., Meyers, P. A., Song, S. R., Kao, S. J., Löwemark, L., et al. (2011b). Variations in monsoonal rainfall over the last 21 kyr inferred from sedimentary organic matter in Tung-Yuan Pond, southern Taiwan. *Quaternary Sci. Rev.* 30, 3413–3422. doi: 10.1016/j.quascirev.2011.08.017

Yao, Y. (1829). Notes for east expedition (in chinese).

Conflict of Interest Statement: The authors declare that the research was conducted in the absence of any commercial or financial relationships that could be construed as a potential conflict of interest.